

LOW-COST DIGITAL DATA TRANSMISSION TECHNIQUE USING FM-RDS PROTOCOL FOR THE AGRICULTURAL SECTOR IN DEVELOPING COUNTRIES

Ndangoh Dam Arantes¹ and Michael Ekonde Sone²

Faculty of Engineering and Technology, University of Buea

ABSTRACT

Existing monitoring systems in developing countries are deficient in detecting diseases and other factors that adversely affect agricultural productivity. This paper presents a low-cost method of disseminating information to farmers by transmitting digital data over an FM channel. The low-cost method is employed in a poultry pen where temperature variations are broadcasted using the radio-text field of the FM-RDS protocol. The system uses a FLIR Lepton 3.5 sensor embedded in a tCam-Mini Rev4 thermal camera to capture temperature values. The FM-RDS transmitter program reads the temperature file every 60 seconds and displays the temperature in the radio-text field of the RDS protocol on an FM station. Differential BPSK is applied to the output of the subband encoder to place the text file on the 57 kHz subcarrier on the FM spectrum. The SDR Touch app decodes the FM-RDS signal using a combination of hardware and software processing. Experimental results show that using the RDS protocol, temperature values could be reliably transmitted with 100% signal quality in a noise-free environment as shown on the advanced RDS features of the SDR Touch app. A signal quality of 95% or more is deemed adequate.

KEYWORDS

Sub band coding, Software-defined radio, FM-RDS, Pi FM transmitter, Thermal imaging.

1. INTRODUCTION

By the end of 2019, research findings showed that 46.4% of the world's population did not have regular access to the internet [1]. Most of this offline population is from developing countries. In addition, the Internet and cellular solutions are still very expensive in these countries, and very few people can afford them.

Several projects have been attempted to extend the internet to remote areas and to connect the unconnected, such as Google Loon [2] using high altitude balloons to provide internet services; Facebook Aquila [3] that uses solar-powered drones flying between 18 to 27km to provide internet services. Both projects failed due to high operating costs and performance issues. More recently, the Starlink project [4], which provides internet access to remote and rural locations globally, using low-earth orbit satellites, is expanding but is still very expensive for users in developing countries. Hence, there is a need to introduce low-cost techniques in developing countries for the dissemination of information in critical areas of the economy, notably in the agricultural sector. One such technique is the use of the FM band for digital data transmission.

The FM band has been underutilized since it has traditionally been dedicated to analog transmission. The FM signal is widespread, with about 70% availability even in developing

countries. Digital data transmission is preferred over analogue data transmission due to its improved resilience to noise, ease of encrypting and decrypting, and easy-to-implement error correction capabilities.

Different techniques of transmitting digital data in the FM band are reported in the literature. In this section, techniques that have a bearing on the low-cost digital data transmission scheme developed in this research will be presented.

The authors in [5] presented two new methods using an FM channel to transmit digital data to mobile terminals. The first method is a modification of the RDS protocol such that only the mono radio signal is used for audio transmission, suppressing the pilot signal and reserving the band from 23 kHz to 76 kHz for data transmission. With this modification, the bandwidth of the RDS protocol is increased from 4.8 kHz to 53 kHz and the bitrate from 1.1875 kHz to 13.1 kHz. The second approach is a modification of the OFDM in which the carriers of each programme are transmitted in one FM channel with a bandwidth of 200 kHz instead of being multiplexed with the carriers of the carriers of other programmes.

In [6] the discrete wavelet transform (DWT) technology is used to compress video data for storage and transmission via an FM channel at 16kbps while retaining a reasonable video quality. In [7] an implementation of the Subsidiary Communication Authorization (SCA) system for the transmission of messages on the FM broadcasting system using FSK modulation on the 67 kHz subcarrier is presented. The baud rate of data delivery and acceptance was set at 600 bps.

In [8] the authors developed an application to warn drivers of potential traffic issues along the highway by transmitting messages in the FM band and using the SDR dongle as a digital receiver. Two different data transmission approaches with different speeds and modulation techniques were employed. The first approach made use of low-speed data transmission on the mono FM radio channel by using QPSK modulation on an 11kHz subcarrier with 8kb/s bit-rate while the second approach deals with high-speed data transmission on the stereo FM radio broadcasting by using QPSK/8-PSK/16-PSK modulation on a 76kHz subcarrier with 40kb/s, 60kb/s and 80kb/s bit-rate respectively.

In this research, we present a novel low-cost digital data transmission technique in the FM band suitable for developing countries by using some of the techniques detailed in [5], [9], [10]. The new scheme will be employed in a poultry farm to assist farmers in real-time monitoring of the activities in the poultry pen. A low-cost local FM transmitter using Raspberry Pi [9] is built to serve as the FM transmitter for images captured at the poultry pen. The system uses a FLIR Lepton 3.5 sensor embedded in a tCam-Mini Rev4 thermal camera to capture temperature values. The FM-RDS transmitter program reads the temperature file every 60 seconds and displays the temperature value in the radio-text field of the RDS protocol on an FM station. Subband coding is later applied to the RDS baseband coding for progressive transmission of data. The subband encoding generator uses BPSK modulation to place the text file on the 57 kHz subcarrier on the FM spectrum. The local transmitter emits warning signals that can be received using an RTL-SDR dongle connected to an RDS-enabled smartphone.

The new method of digital data transmission over an FM band has two advantages over existing methods. First, it is a low-cost digital data transmission to areas in developing countries where access to the internet is difficult. Second, use is made of the wavelet lifting scheme suitable for smartphones with limited memory and a simplified transmitter/ receiver communication system based on SDR.

FM-RDS offers distinct advantages in terms of coverage, cost, and power consumption over alternatives like LoRa, Zigbee, and GSM. Table 1 presents a brief comparison of the above technologies.

Table 1: FM-RDS compared to other transmission technologies

Technology	Coverage	Cost	Power consumption	Use case
FM-RDS	Very wide (regional/national)	Low incremental (uses FM)	Low on the receiver side	Broadcasting info, radio text
LoRa	Long range (2–20 km)	Moderate	Ultra-low (years of battery)	IoT, remote sensing
Zigbee	Short range (10–100 m)	Moderate	Low	Smart home, industrial automation
GSM	Wide cellular coverage	High (network fees)	High	Mobile communication, IoT

FM-RDS is the best option for using the current FM broadcast infrastructure to provide low-cost, wide-area, low-power data (such as text information) to numerous receivers at once. GSM meets mobile, high-data-rate requirements but at a higher cost and power consumption, while LoRa and Zigbee cater to more specialized IoT applications that demand bidirectional communication and device networking. Therefore, FM-RDS is ideal for the wide-scale, low-cost distribution of small data payloads over vast regions, such as temperature or text updates.

The complete outline of the paper is as follows. In the next section, the review of frequency modulation (FM) broadcast is presented. In this section, the basic concepts in the implementation of a stereophonic transmitter/ receiver will be presented. Section 3 presents a review of differential phase shift keying (DPSK), which is a combination of differential line coding and binary phase shift keying (BPSK). In section 4, subband coding based on the factorization of the 4-tap Daubechies filter bank will be reviewed. It will be shown that, though the wavelet transform is an approximate process, a judicious choice of the filter could lead to lossless image processing. RDS baseband coding is presented in Section 5. It will be shown how the captured temperature values are converted to an RDS text file. In section 6, the implementation of the transmitter/receiver is presented. Results and discussions will be presented in Section 7. Finally, the conclusion and recommendations for future research are presented in Section 8.

2. A REVIEW OF FM BROADCAST

The monophonic transmitter could be implemented using the indirect generation based on the Armstrong method. In this method, a Narrow-band FM (NBFM) is converted to a Wide-band FM (WBFM) using frequency converters. Meanwhile, the Monophonic FM receiver is identical to the superheterodyne AM receiver. It consists of an RF (radiofrequency) section, a frequency converter, an intermediate-frequency (IF) amplifier, an envelope detector, and an audio amplifier. In 1961, the FCC approved the transmission of stereophonic sound, which extends the idea of multiplexing signals to generate stereo audio. One of the key requirements of the stereo multiplex signal was to be backward compatible with the large existing base of FM monophonic receivers. To accomplish this goal, the 0 to 15 kHz baseband part of the multiplex (MPX) signal had to contain the left (L) and right (R) channel information (L+R) for monophonic reception. Stereophonic sound is achieved by amplitude modulating the (L-R) information onto a suppressed 38 kHz subcarrier in the 23 to 53 kHz region of the baseband spectrum. A 19 kHz pilot tone is added to the multiplex signal to enable FM stereo receivers to detect and decode the

stereo left and right channels. Today’s MPX signal includes a 57 kHz subcarrier that carries RDS signals

The input, $m(t)$, to the FM monophonic transmitter is a composite (MPX) signal given as

$$m(t) = C_0[L(t)+R(t)] + C_1\cos(2\pi*19\text{kHz}*t) + C_0[L(t)-R(t)]\cos(2\pi*38\text{kHz}*t) + C_2\text{RDS}(t) \cos(2\pi*57\text{kHz}*t) \quad (1)$$

where C_0 , C_1 , and C_2 are gains used to scale the amplitudes of the $(L(t) \pm R(t))$ signals, the 19 kHz pilot tone, and the RDS subcarrier, respectively, to generate the appropriate modulation level. The corresponding spectrum of $m(t)$ is shown in Figure 1.

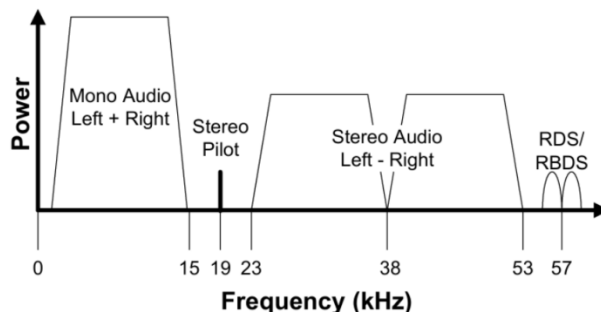


Fig. 1: Composite signal to monophonic transmitter

3. DIFFERENTIAL PSK

Differential PSK (DPSK) signals can be generated by combining two basic operations:

- Differential encoding of the information binary bits
- Phase shift keying

3.1. Differential Line Coding

The differential encoding process starts with an arbitrary first bit, serving as a reference bit, usually symbol 1, initiating the encoding process.

Let $\{m_i\}$ be the input information binary bit sequence, $\{d_i\}$ be the differentially encoded bit sequence. If the incoming bit m_i is “1”, leave the symbol d_i unchanged with respect to the previous bit d_{i-1} . If the incoming bit m_i is “0”, change the symbol d_i with respect to the previous bit d_{i-1}

The reference bit is chosen arbitrarily, here taken as 1

Binary data	1	0	0	1	0	0	1	1	m_i
Differentially encoded binary data	1	1	0	1	1	0	1	1	d_i
	Initial bit								
Transmitted Phase	0	0	π	0	0	π	0	0	0

$$d_i = \overline{d_{i-1}} \oplus m_i$$

Encoding the information in phase difference between successive signal transmissions.

In effect:

- To send “0”, we phase advance the current signal wave form by 180^0
- To send “1”, we leave the phase unchanged

3.2. Binary Phase Shift Keying (BPSK)

In the PSK, the phase is varied to represent binary 1 or 0. Both peak amplitude and frequency remain constant as the phase changes. The phase of the signal during each bit duration is constant, and its value depends on the bit (0 or 1). The bits are associated with a basis function used to distinguish the bits based on the phase difference, π . The signals $s_1(t)$ and $s_2(t)$ associated to the bits are given as

$$\begin{aligned} \text{“1”} &\rightarrow s_1(t) = \sqrt{\frac{2E_b}{T_b}} \cos(2\pi f_c t) \\ \text{“0”} &\rightarrow s_2(t) = \sqrt{\frac{2E_b}{T_b}} \cos(2\pi f_c t + \pi) = -\sqrt{\frac{2E_b}{T_b}} \cos(2\pi f_c t) \end{aligned} \quad (2)$$

$0 \leq t < T_b$, with T_b being bit duration.

f_c : carrier frequency, chosen to be 57 kHz for the RDS modulation

There is one basis function of unit energy

$$\begin{aligned} \phi_1(t) &= \sqrt{\frac{2}{T_b}} \cos(2\pi f_c t) \quad 0 \leq t < T_b \\ s_1(t) &= \sqrt{E_b} \phi_1(t) \quad s_2(t) = -\sqrt{E_b} \phi_1(t) \end{aligned}$$

A binary PSK system is therefore characterized by having a signal space that is one-dimensional (i.e. $N=1$), and with two message points (i.e., $M = 2$)

The corresponding DPSK transmitter obtained by combining differential coding and BPSK is shown in Figure 2

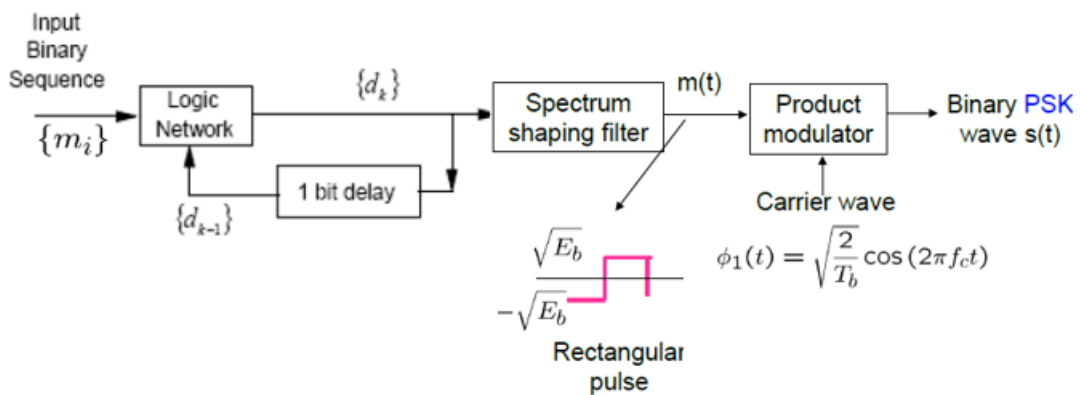


Fig. 2: DPSK transmitter

The equivalent DPSK receiver is shown in figure 3

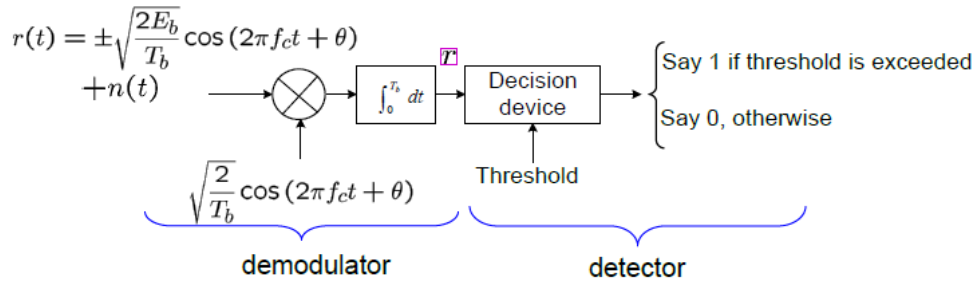


Fig. 3: DPSK receiver

4. SUB BAND CODING [11]

Sub band coding (SBC) is essentially the splitting up of a filter bank into sub bands. A filter bank is a set of filters linked by sampling and delay operators. In [24], [25] it is shown that, the two relationships for perfect wavelet reconstruction for four finite impulse response (FIR) filters are as follows:

$$H_2(z) = H_1(-z) \quad \text{and} \quad H_3(z) = -H_0(-z)$$

The filters are said to be Quadrature Mirror Filters (QMF). $H_2(z) = H_1(-z)$ is called the quadrature mirror filter and if $H_2(z) = z^{-N} H_0(-z^{-1})$ then $H_2(z)$ is called the conjugate quadrature filter of $H_0(z)$.

An example of quadrature mirror filters are two filters

$$H_0(z) = 1 + z^{-1} \quad \text{and} \quad H_1(z) = 1 - z^{-1}$$

which form a QMF pair.

The algorithm for the subband coding involves an iterated filter bank in which the signal is fed into a bank of band-pass filters such that each filter has a bandwidth twice as wide as its left neighbour and a low-pass filter. Hence, subband coding is like a wavelet transform since wavelets give rise to band-pass bands with doubling bandwidth while the scaling function provides the low-pass band. The advantage of subband coding is that only two filters are designed, namely the low-pass and band-pass filters.

The subband coding adopted is the wavelet lifting scheme. It is shown in [10] that, using the wavelet lifting scheme, it is easy to maintain integer values. Lifting is a flexible technique that is applied to the construction of wavelets through an iterative process of updating a subband from an appropriate linear combination of another subband.

The wavelet lifting theorem states that any other finite filter g^{new} complementary to finite filter h is of the form [11], [12]

$$g^{\text{new}}(z) = g(z) + h(z) s(z) \quad (3)$$

where $g^{\text{new}}(z)$, $g(z)$, $h(z)$ and $s(z)$ are Laurent polynomials. For example, the polynomial of filter h is given by

$$h(z) = \sum_{k=k_b}^{k_c} h_k z^{-k} \quad (4)$$

with k_b (respectively k_c) being the smallest (respectively largest) integer number k for which h_k is non-zero. Hence, given a filter h , its complementary filter g^{new} can be found using (3). The odd and even parts of the two filters h and g^{new} are assembled into a matrix called the polyphase matrix $P^{new}(z)$ as follows [11]:

$$P^{new}(z) = \begin{bmatrix} h_e(z) & g_e^{new}(z) \\ h_o(z) & g_o^{new}(z) \end{bmatrix} \quad (5)$$

Factorization of the assembled polyphase matrix of $g^{new}(z)$ and $h(z)$ using lifting steps is performed on a 4-tap Daubechies filter. The factorization of the polyphase matrix is as follows [11], [13], [14].

$$P(z) = \tilde{P}(z) = \begin{bmatrix} 1 & -\sqrt{3} \\ 0 & 1 \end{bmatrix} \begin{bmatrix} 1 & 0 \\ \frac{\sqrt{3} + \sqrt{3}-2}{4} z^{-1} & 1 \end{bmatrix} \begin{bmatrix} 1 & z \\ 0 & 1 \end{bmatrix} \begin{bmatrix} \frac{\sqrt{3}+1}{\sqrt{2}} & 0 \\ 0 & \frac{\sqrt{3}-1}{\sqrt{2}} \end{bmatrix} \quad (6)$$

(6) forms the basis of the integer-to-integer wavelet transform used in implementing the new cryptosystem. A 4-tap Daubechies filter bank was preferred to other filter banks since it has a scaling factor close to unity [11], [12]. The forward transform using the integer version of the primal and dual lifting steps is computed using the odd and even samples of the residue sequence, x as follows

$$\begin{aligned} |a_n|_{m_j} &= \left\| \left\| x_{2l} h_1|_{m_j} + x_{2l+1} h_2|_{m_j} \right\| + x_{2l+1} \right\|_{m_j} \\ |d_n|_{m_j} &= \left\| \left\| x_{2l} h_1|_{m_j} + x_{2l+1} h_2|_{m_j} \right\| + a_{n-1} \right\|_{m_j} \end{aligned} \quad (7)$$

where $h_1 = -\sqrt{3}$; $h_2 = \frac{\sqrt{3}}{4}$; $h_3 = \frac{\sqrt{3}-2}{4}$ and a_n and d_n are the approximation and detail sequences of wavelet coefficients of the n th residue. For a given modulus, the message sequence is converted to integer versions of the first-level approximation and detail wavelet coefficients using (7). The first level k th detail and approximation wavelet coefficients are denoted, respectively, as d_k^1 and a_k^1 with $1 \leq k \leq N/2$ where N is the original number of samples.

Also using (7) and downsampling by 2, the first-level approximation coefficients, a_k^1 are transformed to the second level approximation and detail coefficients denoted as d_k^2 and a_k^2 with $1 \leq k \leq N/4$. Meanwhile, the first-level coefficients, d_k^1 are sent to the differential phase shift keying block.

The process for the first two levels of decomposition is shown in the synopsis of Figure4, with processing elements (PEs) used in the computation of (7).

For the first level decomposition, the input to the processing block is N datapoints, and the corresponding output is d_k^1 and a_k^1 with $N/2$ data points for a given modulus. For the second and higher levels of decomposition, the input to the processing block are previous values of the approximation coefficients, a_k^{n-1} for the n th decomposition level with $2 \leq n \leq N/4 - 1$ and the output coefficients are d_k^n and a_k^n with $N/2^n$ datapoints and $1 \leq k \leq N/2^n$ [11].

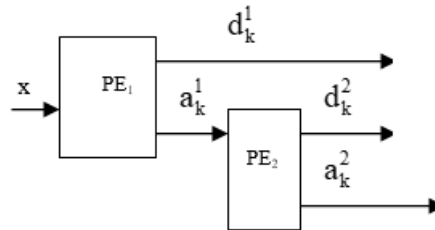


Fig.4: Synopsis for the computation of the k th coefficients for the 1st and 2nd levels of decomposition

The final decomposition level will have only one datapoint. The processing of this datapoint will give one approximation coefficient and one detail coefficient.

The first stage of the forward transform is depicted in Figure 5, where H_0 is a low-pass filter and H_1 is a high-pass filter. The $(\downarrow 2)$ symbol represents downsampling by 2, which means that every other sample is thrown away. The 1st, 3rd, 5th, - - - samples are kept and the 2nd, 4th, 6th, - - - samples are discarded. Starting with 16 samples, $a(n)$ and $d(n)$ contain 8 samples each.

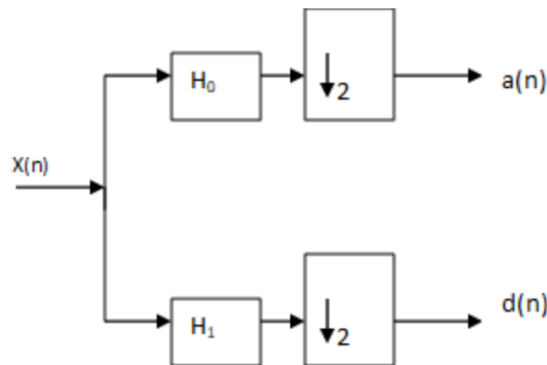


Fig. 5: The first stage of the wavelet forward transform

To find the inverse transform, the process is reversed. The process starts with the approximation and detail coefficients a_0 and d_0 , respectively, obtained at the final decomposition level of the forward transform. The first stage of the inverse transform is shown in Figure6 [11].

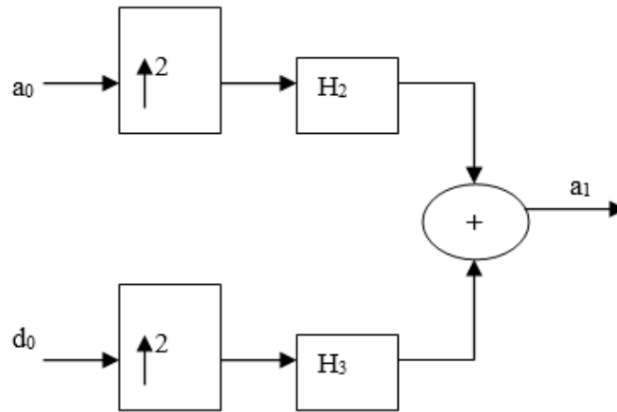


Fig. 6: The first stage of the inverse transform

The $(\uparrow 2)$ symbol represents upsampling by 2, which means that zeros are inserted between samples, while H_2 and H_3 are the filter coefficients used in (7). The inverse transform is computed using (7) by reversing the processing for the forward transform and flipping signs [11]. The $(\uparrow 2)$ symbol represents upsampling by 2, which means that zeros are inserted between samples. Starting with a signal of length 4 given by $\{1, 2, -1, 3\}$, the resulting upsampled signal is $\{1, 0, 2, 0, -1, 0, 3, 0\}$, which has length 8. Initially, there is one sample at the input of each upsample-filter branch, the output will contain two samples. For proper filters H_2 and H_3 , the output of the first summer will be $a_1(n)$. Figure 2.5 shows the first two stages of the inverse transform.

This process continues until the last output is $x(n)$, the original signal. Note that $a_0(n)$, $d_0(n)$, $d_1(n)$, $d_2(n)$, $d_3(n)$ must be supplied at successive stages of this process. These are the terms that were saved and called the transform in the forward process.

The inverse process continues until the last output is $x(n)$, the original residue sequence that was fed into the subband encoder. Note that the approximation coefficients, $a(n)$, and the detail coefficients, $d(n)$ must be supplied at successive stages of the inverse process. These coefficients obtained from the forward process are stored in registers as depicted in Figure 7 [11], [15].

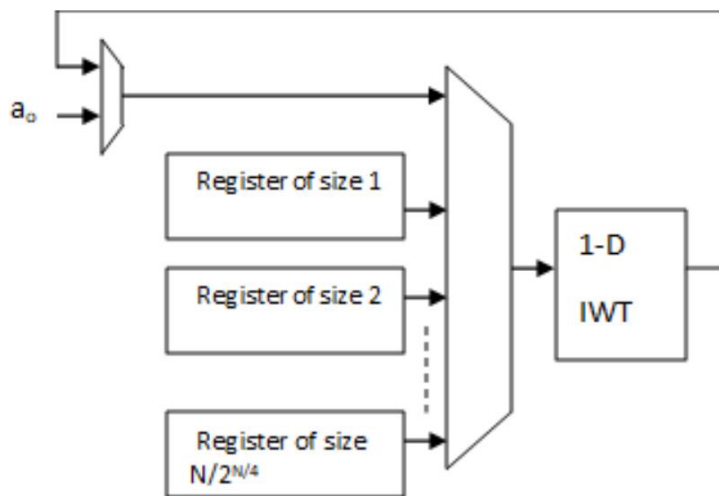


Fig.7: Block diagram of the subband decoder

5. RDS BASEBAND CODING

RDS is a mature technology; the first official standard was published in 1984 [16]. RDS baseband coding refers to the formatting and encoding of digital data for transmission over an FM channel. The coding scheme is organized into groups and blocks, each consisting of four blocks of 26 bits long. The total length of a group is 104 bits. One block consists of a 16-bit information word and a 10-bit CRC check word, which is added for error detection and correction. Figure 8 shows the structure of RDS baseband coding.

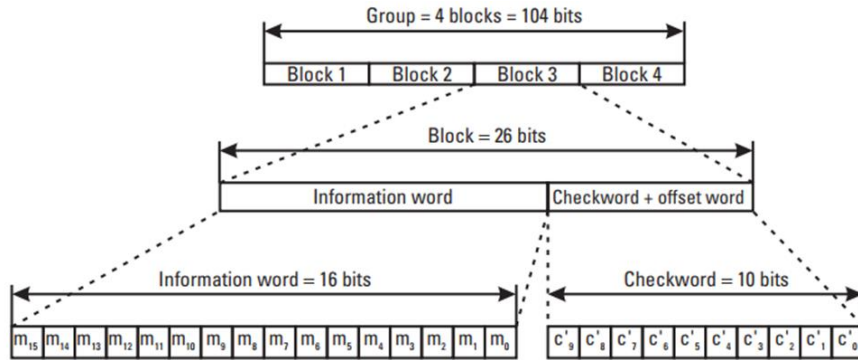


Fig. 8: Structure of RDS baseband coding [16]

The RDS baseband coding is applied to temperature values captured using the FLIR Lepton 3.5 sensors at various points in the poultry pen. The different temperature values are transmitted progressively to fit into the FM band reserved for digital transmission. The different stages involved in the processing of the captured temperature values are shown in Figure 9.

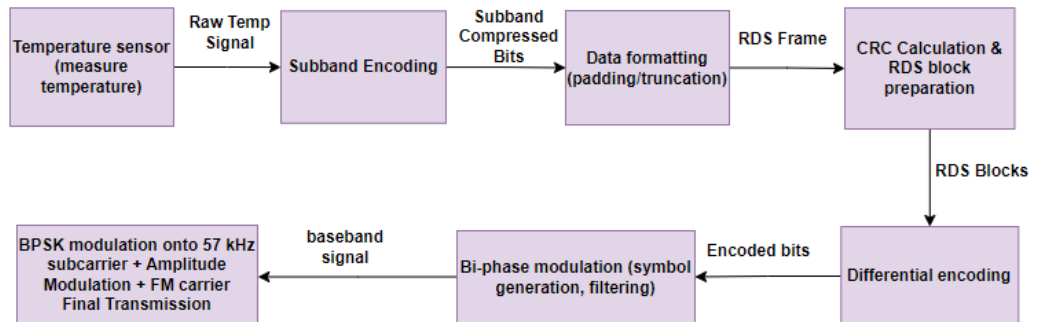


Fig. 9: Processing stages at the transmitter

The compressed temperature data is mapped into the radio text field (group 2A) of RDS using ASCII encoding. The measured temperature values are transmitted progressively using the subband encoding stage, for example, using eight (08) initial temperature datapoints; four (04) are transmitted, later two (02), and finally one (01) detail and one (01) approximate datapoint. The datapoints are formatted into an ASCII string, for example, $23.5\text{ }^{\circ}\text{C} \rightarrow \text{ASCII} = 32\ 33\ 2\text{E}\ 35\ \text{B0}\ 43$, ensuring that the string does not exceed the RDS radio text (RT) character limit of 64.

RDS uses a 57 kHz subcarrier locked to the third harmonic of the FM stereo pilot tone (19 kHz) to send data at 1,187.5 bits per second. Bitstreams are transformed into self-clocking signals using differential encoding, which combines clock and data information to facilitate

synchronization. The encoded baseband signal using BPSK modulates the 57 kHz subcarrier at double the bitrate, yielding a symbol rate of 2375 baud. The other steps involved in the processing of the datapoints at the transmitter are outlined as follows:

- A 16-bit information word composed of two ASCII characters (8 bits each, MSB-first), and a 10-bit CRC error-checking code that uses the polynomial $x^{10} + x^8 + x^7 + x^5 + x^4 + x^3 + 1$, are formed;
- Offset word: A, B, C, or D is used to identify block position. Four blocks are combined into a 104-bit group such that
 - Block 1: 32 33 + CRC + Offset A
 - Block 2: 2E 35 + CRC + Offset B
 - Block 3: B0 43 + CRC + Offset C
 - Block 4: Padding + CRC + Offset D
- The bits are transmitted starting with the most significant bits (MSB-first) within each 16-bit word. The bits are transmitted at 1187.5 bps, which is the RDS subcarrier frequency of 57 kHz divided by 48.
- BPSK is used to modulate data onto the 57 kHz subcarrier, which is the third harmonic of the 19 kHz pilot tone to ensure compliance with FM standards.

At the receiver, the entire process is reversed as shown in Figure 10.

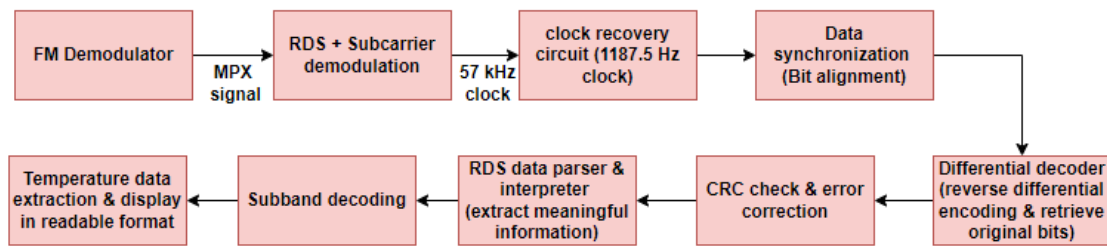


Fig. 10: Processing stages at the receiver

It was worth noting that there is a buffer at the receiver used to reassemble the datapoints from the transmitter through progressive transmission shown in Figure 6.

6. IMPLEMENTATION OF TRANSMITTER/ RECEIVER OF THE STEREOPHONIC SIGNAL

In this section, the implementation of the transmitter/ receiver model as applied to Smart Poultry Monitoring using the FM-RDS protocol is presented.

Thermal imaging cameras, the tCam-Mini Rev4 model, with good resolution, high sensitivity, and data export capabilities, are used. The cameras are mounted upon a tripod and positioned in different areas where they can scan at least three-quarters of the poultry pen. The camera communicates wirelessly with Raspberry Pi model 3B for data storage and processing. The tCam-Mini Rev4 comes pre-calibrated, except for the emissivity coefficient, which could be altered. The emissivity coefficient of the camera was set at 0.95, which is the generally agreed-upon value by researchers working with biological material [17]. The system is configured to monitor the temperature in the poultry pen in real-time and send temperature values and images to the Raspberry Pi for storage. The Raspberry Pi is configured as an FM-RDS transmitter, transmitting the measured temperatures via the RDS radio text field every minute.

6.1. FM-RDS Transmitter

Hardware:

The Raspberry Pi model 3B can be configured as an FM-RDS transmitter by connecting a simple wire to the GPIO (General Purpose Input/Output) pin 4 to create an antenna. The Raspberry Pi uses the GPIO pins to generate FM signals.

The output capabilities of a Raspberry Pi's GPIO pin set a limit on the transmitter's transmission power. It can produce up to 50mA of current and has a maximum output voltage of 3.3V. As a result, 165 mW is the highest potential transmission power. Figure 11 shows the basic parts of the Raspberry Pi and the tCam camera.

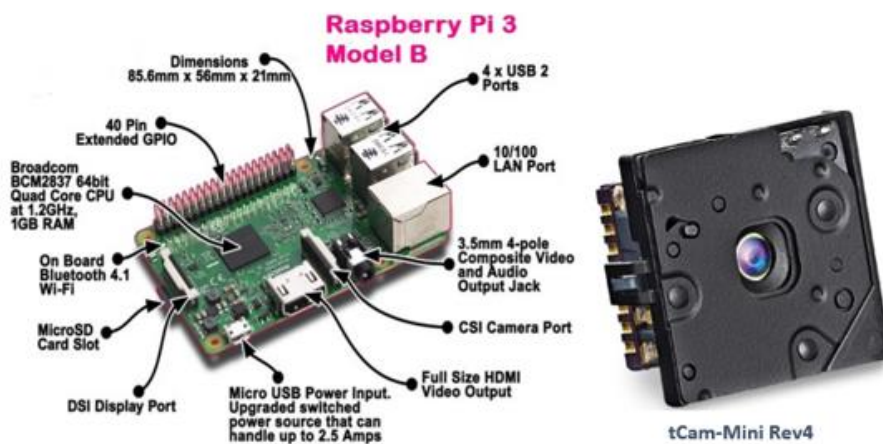


Fig.11: Raspberry Pi and tCam-MiniRev4 thermal camera

The tCam-Mini is a small, ESP32-based wireless streaming thermal imaging camera designed to provide radiometric data from a Flir Lepton 3.5 sensor [18]. It requires a 5V power supply with at least 500mA of current.

Software

- SDR driver app
- SDRTouch app to receive FM_RDS on a smart phone
- tCam-Mini desktop application

To install Pi-FM transmitter program, we clone the github repository github.com/ChristopheJacquet/PiFmRds [19] into the root directory on Raspberry pi.

The FM-RDS transmitter application runs on the Raspberry Pi model 3B, which is used for the hardware/software implementation. The SDR Touch app is used to perform the decoding in software. The RTL-SDR USB dongle and an Android phone's USB host capabilities are used by the SDR Touch app to decode FM-RDS signals through a combination of hardware and software processing. A USB OTG cable is used to connect the RTL-SDR dongle to a Samsung Galaxy A20 model. Raw RF signals between 20 MHz and 1.75 GHz, including the FM range 87.5–108 MHz, can be recorded by the RTL-SDR dongle. The 57 kHz RDS subcarrier and the FM station's primary audio carrier are separated using the SDR Touch app. The RDS data is taken out of the subcarrier by a quadrature demodulator. The 1187.5 Hz clock signal that is included in the

transmission is used to identify RDS data groups. After that, the groups are verified by CRC code error-checking. After extraction, the temperature data is displayed.

6.2. Pi-FM-RDS Program design

The `rds.c` file contains the RDS data generator, which creates one 2A group for Radio Text (RT) transmission and four 0A groups for PS transmission. The modulation used is Binary Phase Shift Keying (BPSK). To collect RDS data samples, call the `get_rds_samples` function, which then calls the `get_rds_group` function. This method creates a biphasic symbol and differentially encodes the signals. The effect of making successive biphasic symbols overlap is equivalent to applying a root-raised-cosine (RRC) filter, a pulse-shaping filter, on a series of Manchester-encoded pulses. The program samples internally at 228 kHz, which is four times the 57 Hz RDS subcarrier frequency. The `fm_mpx.c` file upsamples the input audio file to 228 kHz to generate the FM multiplex signal baseband. The stereo pilot tone at 19 kHz, the left-right signal amplitude modulated on the 38 kHz suppressed carrier, the RDS signal from `rds.c`, and the left + right signal band limited to 15 kHz make up the FM multiplex signal. A zero-order hold and a 60 FIR low-pass filter are used to produce the upsampling. A Hamming window creates a sinc window in the filter. To cut frequencies higher than the Nyquist frequency minimum, the filter coefficients are created at startup. The `pi_fm_rds.c` file, which was modified from Richard Hirst's PiFMDma [20], plays the samples.

The transmitting program reads temperature data every minute from a file on the server and updates the RDS radio text field.

6.3. Experimental Setup

FM monophonic transmitter receives a composite (MPX) signal as input, $m(t)$ given in (1) section 2. Figure 12 shows a conceptual block diagram of an MPX encoder used to generate the MPX signal, $m(t)$.

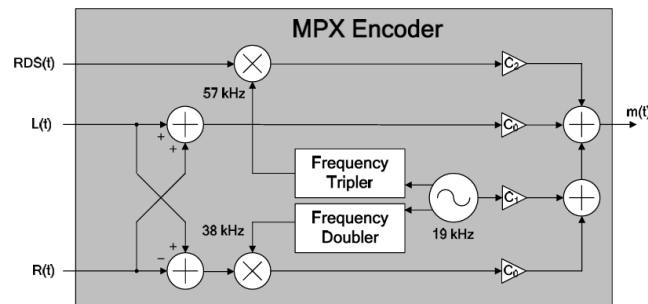


Figure 12: Block diagram of an MPX encoder

The composite signal $m(t)$ is fed into the Raspberry Pi which functions as an FM transmitter. A WLAN is set up to ease communication between the thermal camera, the server and Raspberry pi. The thermal camera and the Raspberry Pi are assigned static IP addresses.

The monitoring and transmitting unit are shown in Figure 13. It consists of a tCam-Mini Rev 4 thermal camera, a Raspberry Pi board acting as an FM transmitter, and a 5000 mAh battery.

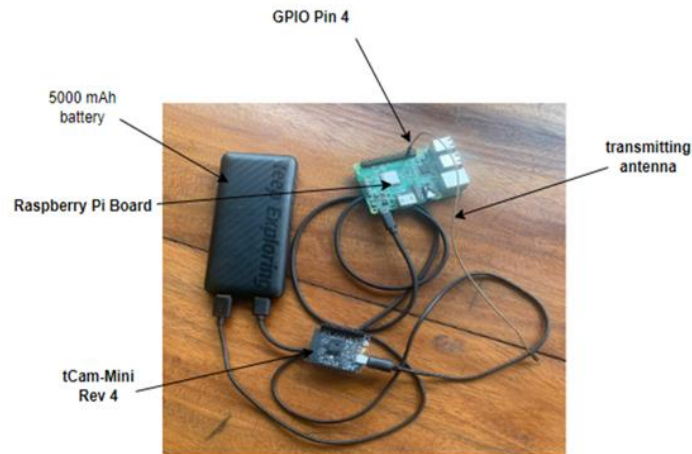


Fig. 13: Monitoring and Transmitting unit

6.4. FM-RDS Receiver

Figure 14 below shows a conceptual block diagram of an MPX decoder used to recover the left, right and RDS signals from the MPX message signal, $m(t)$.

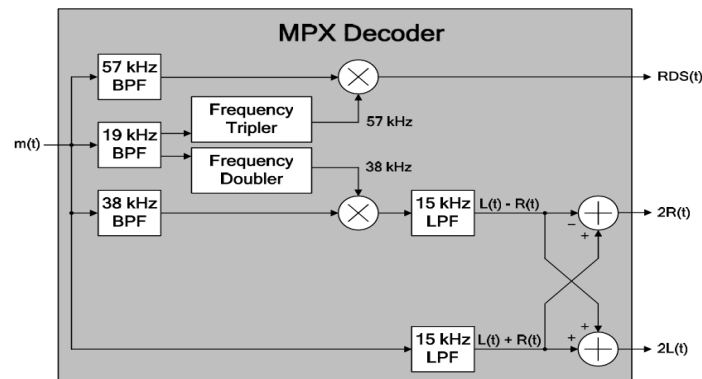


Figure 14: Block diagram of an MPX decoder

The message signal is applied to three bandpass filters with center frequencies at 19, 38, and 57 kHz and to a low-pass filter with a 3-dB cutoff frequency of 15 kHz. The 19 kHz bandpass filter is a high-Q filter used to extract the 19 kHz pilot tone from the MPX message signal. The recovered pilot tone is frequency-doubled and tripled to produce the required local oscillator (LO) signals needed to demodulate the (L-R) and RDS signals, respectively. By adding and subtracting the (L+R) and (L-R) signals, a scaled version of the left and right channels is recovered for stereophonic sound. RDS is brought back down by mixing with a 57 kHz LO, and the data can be recovered by sending this signal to a matched filter. In our work, we use a software-defined radio device to receive and decode the MPX signal by using a smartphone and the SDR-RTL dongle. The RTL-SDR driver and the SDRTouch app are installed on the smartphone. The dongle drive is connected to the phone through an OTG (On the Go) adapter. The SDR Touch app supports receiving FM radio and decodes any associated RDS data as shown in Figure 15.

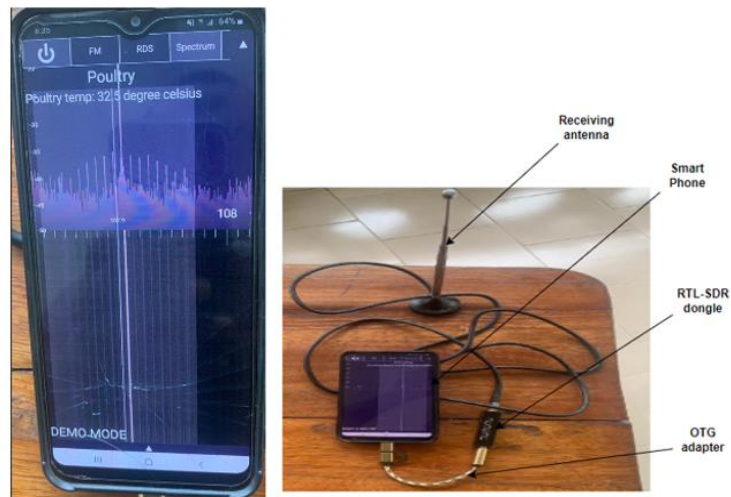


Fig. 15: Receiver unit

Figure 14 shows the basic building components of the receiver and display of a captured temperature value of 32.5⁰C on the smartphone.

7. RESULTS AND DISCUSSIONS

Thermal videos of the poultry pen are streamed via a wireless interface with the camera using the tCam-Mini desktop application. The software offers temperature indicators at various locations as well as a graphing tool to show how temperatures change over time. Real-time monitoring of the poultry pen is depicted in Figure 16, along with the temperature at the spot meter and three other locations.

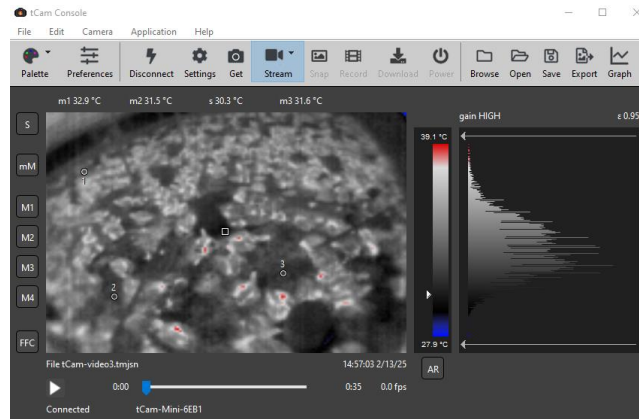


Figure 16: Temperature at different points in a poultry pen as displayed on tCam desktop application

Figure 17 illustrates the use of the graphing capability offered by the tCam-Mini desktop application to visualize the temperature variation at the points marked with markers. A file in text format contains the temperatures at the locations marked using markers. The Raspberry Pi FM transmitter program reads changing temperature data from this file and transmits it via the radio-text field of the FM-RDS protocol.

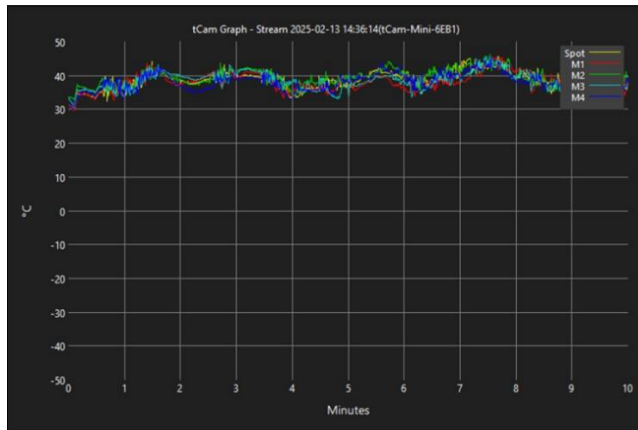


Fig. 17: Graph showing temperature variation at different points indicated with markers in the poultry pen over time

The SDR Touch app, together with the SDR Touch key, displays constellation diagrams and RDS group data. It also displays a spectrum analyzer for visualizing the FM-RDS signal and signal quality indicators, as shown in Figure 18.

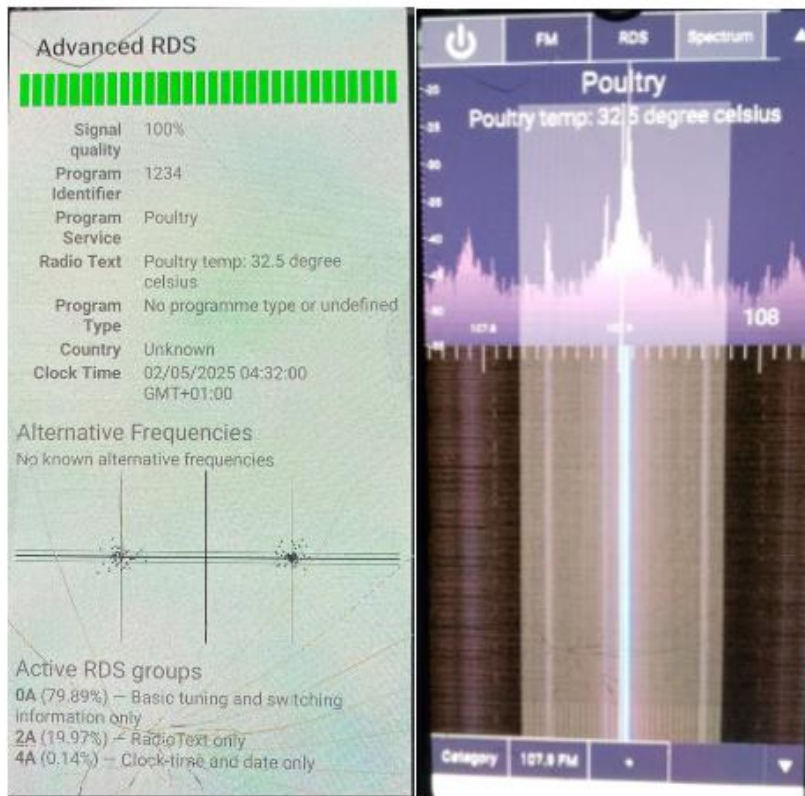


Fig.18: FM-RDS signal quality indicators and spectrum

Measuring a real-time system's bit error rate is challenging. Our system's transmission dependability is assessed by looking at the sophisticated RDS characteristics that are visible on the SDR Touch receiver app. We can learn enough about the successful frame decoding rate from the BPSK constellation diagram and the signal quality. 95% or higher signal quality is considered satisfactory.

8. CONCLUSION AND FUTURE WORK

Using the FM-RDS protocol, we have created and put into place a system to track and broadcast the temperature in a poultry pen. A Samsung phone linked to the RTL-SDR dongle receives the temperature readings, which are broadcast on the FM-RDS's radio-text field. The focus was on real-time poultry monitoring system so that a chicken head region identification algorithm, like YOLO [21] (You Only Look Once), can identify the chicken's head region and assess the temperature there. The YOLO algorithm recognizes the area of the chicken's head and provides markers so that the tCam-Mini thermal camera may measure the temperature at the designated areas. This improvement will significantly speed up the process of identifying sick or deceased chickens. In other agricultural applications, this method can be quite effective at broadcasting sensor data. In our future work, data can be safeguarded by using an encryption/decryption scheme because radio transmission is intended for all listeners.

REFERENCES

- [1] I. del Portillo, S. Eiskowitz, E. F. Crawley, and B. G. Cameron, "Connecting the other half: Exploring options for the 50% of the population unconnected to the internet," *Telecommun. Policy*, vol. 45, no. 3, p. 102092, Apr. 2021, doi: 10.1016/j.telpol.2020.102092.
- [2] P. Serrano, M. Gramaglia, F. Mancini, L. Chiaraviglio, and G. Bianchi, "Balloons in the Sky: Unveiling the Characteristics and Trade-Offs of the Google Loon Service," *IEEE Trans. Mob. Comput.*, vol. 22, no. 6, pp. 3165–3178, Jun. 2023, doi: 10.1109/TMC.2021.3135976.
- [3] F. A. d'Oliveira, F. C. L. de Melo, and T. C. Devezas, "High-Altitude Platforms — Present Situation and Technology Trends," *J. Aerosp. Technol. Manag.*, vol. 8, pp. 249–262, Sep. 2016, doi: 10.5028/jatm.v8i3.699.
- [4] "Starlink satellite project impact on the Internet provider service in emerging economies," *Res. Glob.*, vol. 6, p. 100132, Jun. 2023, doi: 10.1016/j.resglo.2023.100132.
- [5] M. J. de-Ridder-de-Groote, R. Prasad, and J. H. Bons, "Analysis of new methods for broadcasting digital data to mobile terminals over an FM-channel," *IEEE Trans. Broadcast.*, vol. 40, no. 1, pp. 29–37, Mar. 1994, doi: 10.1109/11.272418.
- [6] "Video compression transmission via FM radio." Accessed: Jul. 27, 2024. [Online]. Available: <https://www.spiedigitallibrary.org/conference-proceedings-of-spie/4391/0000/Video-compression-transmission-via-FM-radio/10.1117/12.421226.full>
- [7] "SCA system (Subsidiary Communications Authorization) Implementation of Text Transmission on Broadcasting System - Diponegoro University | Institutional Repository (UNDIP-IR)." Accessed: Aug. 01, 2024. [Online]. Available: <http://eprints.undip.ac.id/106/>
- [8] R. G. Bozomitu, F. D. Hutu, and N. De Pinho Ferreira, "Drivers' Warning Application Through Image Notifications on the FM Radio Broadcasting Infrastructure," *IEEE Access*, vol. 9, pp. 13553–13572, 2021, doi: 10.1109/ACCESS.2021.3050669.
- [9] R. W. Stewart, K. W. Barlee, and D. S. W. Atkinson, *Software Defined Radio using MATLAB & Simulink and the RTL-SDR*. Glasgow, GBR: Strathclyde Academic Media, 2015.
- [10] A. Eden, "Your Guide to FM RDS: What Is It, and How Does It Work?," Media Realm. Accessed: Nov. 06, 2024. [Online]. Available: <https://www.mediarealm.com.au/articles/fm-rds-radio-data-system-guide/>
- [11] Sone, M.E., "Efficient Key Management Scheme To Enhance Security-Throughput Trade-Off Performance In Wireless Networks". In Proc. Science and Information Conference (SAI), London, UK, July 28-30 2015, pp. 1249 – 1256
- [12] W. Sweldens, "The lifting scheme: A construction of second generation wavelets". Siam J. Math. Anal, vol.29, No. 2 (1997). Preprint, 1996.
- [13] I. Daubechies and W. Sweldens, "Factoring Wavelet Transforms into lifting steps". J. Fourier Anal. Appl., vol. 4 Nr. 3, 1998.Preprint.
- [14] M.J. Mashen, "Factoring wavelet transforms into Lifting steps" University of Australia, 1997 Circuits and Systems (ISCAS 2004), vol. 2, 2004, pp. 667 – 700.

- [15] Ningo, N.N. and Sone, M.E (2010), 'Efficient key management FPGA-based cryptosystem using the RNS and iterative coding', *Int. J. Information and Communication Technology*, Vol. 2, No. 4, pp. 302 - 322
- [16] D. Kopitz and B. Marks, *RDS, the radio data system*. Boston: Artech House, 1999.
- [17] I. A. Nääs, R. G. Garcia, and F. R. Caldara, "Infrared Thermal Image for Assessing Animal Health and Welfare," *J. Anim. Behav. Biometeorol.*, vol. 2, no. 3, pp. 66–72, Jul. 2014, doi: 10.14269/2318-1265/jabb.v2n3p66-72.
- [18] "tCam-Mini: An ESP32-Based Radiometric Thermal Imaging Camera - Hackster.io." Accessed: Feb. 17, 2025. [Online]. Available: <https://www.hackster.io/dan-julio/tcam-mini-an-esp32-based-radiometric-thermal-imaging-camera-096308>
- [19] J. Miegler, *miegler/PiFmAdv*. (Nov. 05, 2024). C. Accessed: Nov. 21, 2024. [Online]. Available: <https://github.com/miegler/PiFmAdv>
- [20] "PiBits/PiFmDma at master · richardghirst/PiBits," GitHub. Accessed: Jan. 03, 2025. [Online]. Available: <https://github.com/richardghirst/PiBits/tree/master/PiFmDma>
- [21] L. Syafaah, A. Faruq, and N. Setyawan, "Sick and Dead Chicken Detection System Based on YOLO Algorithm," *Ingénierie Systèmes D'Information ISI J.*, vol. 9, no. 25, Art. no. 25, 2024, Accessed: Feb. 13, 2025. [Online]. Available: <https://www.iieta.org/journals/isi/paper/10.18280/isi.290506>

AUTHORS

Michael Ekonde Sone is an Associate Professor in Telecommunications and Networks Security. He is currently the Deputy Vice-Chancellor at the University of Buea, Cameroon. His research interests are principally in designing communication systems that enhance both security and throughput at the physical, data link, and network layers of the TCP/IP model. To achieve this feat, he developed a novel cryptographic algorithm that combines wavelet lifting scheme (subband coding), non-linear convolutional coding, and RSA public-key cryptography. He has published extensively in peer-reviewed journals and contributed book chapters in books on cybersecurity, notably *New Perspectives in Behavioral Cybersecurity* by Wayne Patterson and *Computer and Network Security* by J. Sen.



Ndangoh Dam Arantes is a final year PhD student at the faculty of engineering and technology, University of Buea, Cameroon. His PhD is in the field of Telecommunications and Networks. His research interests include designing digital data communication systems for the FM band, Modulation techniques for efficient bandwidth management, Software-defined radio and its applications. He has published a conference paper captioned "Simulation framework for data transmission by FM broadcasting on a two-ray propagation channel".

